Available online at scholarcommons.usf.edu/ijs

International Journal of Speleology

Official Journal of Union Internationale de Spéléologie

The affordable DIY Mandeye LiDAR system for surveying caves, and how to convert 3D clouds into traditional cave ground plans and extended profiles

Loris Redovniković [1], Antun Jakopec [2], Janusz Będkowski [3], and Jurica Jagetić [1]

[1]Faculty of Geodesy, University of Zagreb, Kačićeva 26, 10000 Zagreb, Croatia
[2]SLAM Geodezija Ltd., Ulica Bože Težaka 1A, 42000, Varaždin, Croatia
[3]Institute of Fundamental Technological Research Polish Academy of Sciences, Pawińskiego 5B, 02-106 Warsaw, Poland

Abstract: The paper examines the potential use of low-cost LiDAR for cave surveying. Mobile mapping using LiDAR complements traditional speleological surveying using a polygonal traverse. These methods assist each other, with one serving as an independent control measurement for the other, ultimately resulting in a more accurate 3D model. The testing results show that achieving high accuracy and detailed cave representation is possible using open hardware and open-source software. Both spacious and well-indented cave sections and narrow passages barely passable by humans were successfully mapped. The surveying process is significantly faster than traditional cave mapping, as drawing cave sketches by hand is unnecessary, being the most time-consuming task on site. This paper also presents a procedure for automated ground plan generation and profile generation from 3D point clouds, further expediting and simplifying the work for speleologists using scanning systems. Also, it is confirmed that the results are reproducible and do not depend on the subjective interpretation of the cartographer, as is the case with traditional speleological drawings.

Keywords: Cave mapping, mobile laser scanning, open hardware, open-source software, cave profiles

Received 12 October 2024; Revised 6 January 2025; Accepted 10 January 2025

Citation: Redovniković, L., Jakopec, A., Będkowski J., Jagetić, J., 2024. The affordable DIY Mandeye LiDAR system for surveying caves, and how to convert 3D clouds into traditional cave ground plans and extended profiles. International Journal of Speleology, 53(3), ijs2535. https://doi.org/10.5038/1827-806X.53.3.2535

INTRODUCTION

Caves have long played an important role in human history, serving as shelters and protection from harsh weather or enemies. While they no longer hold the same practical significance for humans, caves continue to evoke a sense of awe and remain challenging environments for exploration. Their harsh conditions, including darkness, dampness, and sometimes cold temperatures, make them some of the least-explored places on Earth and unique and promising places for researchers.

Speleologists, driven by a passion for exploration and discovery, venture into these hidden corners of the Earth, often navigating narrow and low passages. One of the essential activities during cave exploration is conducting topographical surveys and representing these findings on maps. Despite technological advances, cave surveying remains a highly complex and time-consuming activity, requiring specialized surveying equipment and methods tailored to the unique conditions of caves.

CAVE SURVEYING

Traditional underground surveying methods used compasses, clinometers, and measuring tapes (White, 2019). Caves were mapped on-site on graph paper and later copied more neatly for better legibility. The most important data was a table containing traverse lines marked on site. In challenging cave conditions, errors in measurements and data recording were common, as were later mistakes during data transferring. Today, laser rangefinders are commonly used for cave surveys, equipped with an additional chip that stores distance, azimuth, and inclination angle directly into built-in memory. The most well-known device was DistoX (Heeb, 2009), later replaced by DistoX2 (Heeb, 2014; Konstantinos, 2018). Since both devices are now discontinued, alternatives such as DistoXBLE (Tian, 2023) and BRIC5 (BRIC Survey Tool, n.d.) are currently available. Software tools can also transfer the data from those devices and make a visual representation on mobile or tablet screens. One of the most widely used applications for field cave mapping

*loris.redovnikovic@geof.unizg.hr

The author's rights are protected under a Creative Commons Attribution-NonCommercial 4.0 International (CC BY-NC 4.0) license.

today is TopoDroid (Corvi, n.d.). After collecting the field data, they can be exported in various formats. The data can be further processed in different software programs. Therion (Therion Development Team, n.d.) is particularly notable, offering an extensive range of capabilities. Such an automated data collection and processing method reduces the chance of errors. However, mistakes can still occur due to carelessness, measuring near metal objects, or using uncalibrated equipment. Despite all these advances, cave surveying remains a demanding and time-consuming task that requires considerable effort. Therefore, laser scanning is a technology that could significantly speed up and simplify this process.

LASER SENSORS FOR UNDERGROUND SURVEYING

The laser is a particularly suitable sensor for underground surveying since it does not require lighting; most of them work better in darkness than in sunlight. Laser devices can be 1D, 2D, or 3D. 1D sensors measure length only in one direction. An example of how a good 3D model of a cave can be obtained with a 1D sensor through a lot of effort and expertise is described in Gáti et al. (2016).

By rotating a 1D sensor around an axis perpendicular to the direction of length measurement and knowing the angular displacement per unit of time, we obtain 2D rotational scanners, also known as 2D lidars. A recent study by Tringali et al. (2024) describes using 2D lidars in cave surveying.

If a 2D LiDAR rotates around the horizontal axis, and the entire system rotates around the vertical axis, we get a 3D static scanner. Static laser scanning provides precise results but requires more time for site scanning and subsequent data processing, which includes registering scans into a coherent point cloud and georeferencing the point cloud to place it in the correct coordinate system. Several studies explore the processing of point clouds obtained from static laser scanning of caves, particularly emphasizing free software solutions. Notable examples include Silvestre et al. (2015), Šupinský et al. (2022), and Kaňuk et al. (2023).

Besides static laser scanning, dynamic laser scanning is also available, and if additional sensors are integrated, then we talk about a mobile mapping system. Dynamic scanning is generally somewhat less accurate than static scanning, but it offers increased mobility and faster surveying. An example where several such systems were compared for the measurement of an underground object can be found in Trybała et al. (2023). The study by Zlot and Bosse (2014) also describes mobile cave mapping, while Sevil-Aguareles et al. (2025) demonstrate the integration of traditional mapping with laser scanning for gypsum cave studies. One of the main reasons why mobile mapping has not gained broader adoption in cave surveying is the high cost of such systems.

One limitation of dynamic real-time scanning is the accumulation of errors during a prolonged scanning period. This issue is especially problematic in complex cave environments. In such cases, relying on post-processing techniques and georeferencing using points gathered through more reliable methods is mandatory.

It was previously mentioned that, in addition to 2D rotating scanners, there are also 3D rotating scanners. Initially, they were made by vertically stacking multiple 2D rotating scanners, one below the other. In practice, 3D rotating scanners with 16, 32, 64, and 128 channels have been commonly used, with some systems offering even fewer or more channels depending on specific applications. Increasing the number of channels enhances the density and detail of the resulting point cloud but also significantly raises the cost.

Rotational components are complex to manufacture, which has kept the price of rotational 3D scanners relatively high. As a result, they have not been commonly used in caves. Additionally, moving parts in these scanners are delicate and prone to damage, especially in demanding environments like caves. This is particularly critical for 3D LiDARs, which include more moving parts than their 2D counterparts, increasing the risk of failure. Combined with their high price, this makes such systems impractical for widespread use in cave surveying. Therefore, low-cost, robust solutions are necessary to make this technology viable.

However, in recent years, solid-state LiDARs based on chip technology have been developed, allowing mass production at significantly lower prices (Li et al., 2021). These inexpensive solid-state LiDARs will have extensive applications in many human activities in the future, including cave surveying.

As previously mentioned, technological advancements have reduced both the cost and size of the hardware and improved software quality, some of which are free. The Mandeye system, for example, can be configured to mount easily on a helmet or shoulder, enabling hands-free exploration and seamless 3D documentation of caves. This paper will explore the capabilities of the Mandeye system for mobile cave mapping.

MANDEYE LIDAR SYSTEM

The Mandeye LiDAR name is inspired by a combination of “Mandala,” symbolizing completeness and balance, and “Eye,” representing human perception and vision. This name reflects the system's purpose—to offer a comprehensive and balanced solution for affordable mobile mapping, drawing inspiration from human sensory perception.

The system's development was a collaborative effort. Janusz Bedkowski led the software development (Bedkowski, 2022a, b), while Michał Pełka contributed significantly to the hardware design (Będkowski, 2023). Their combined expertise resulted in a solution that is innovative, accessible, and highly efficient for a wide range of users.

Hardware overview

The Mandeye system is built around the Livox Mid-360 hybrid solid-state LiDAR sensor, which offers excellent durability and range at an affordable price.

While the Mid-360 sensor is primarily designed for service robots operating in controlled environments like warehouses, restaurants, or houses, it offers an IP67 rating. It is fully protected against dust and can withstand immersion in water up to 1 meter for 30 minutes. This makes it resilient to challenging cave conditions such as humidity, dust, water droplets from ceilings, and minor impacts. The specifications also state that the minimum range of the Livox Mid-360 sensor is 0.1 m, while the maximum range is 40 m at 10% reflectivity and up to 70 m at 80% reflectivity.

The system is powered by direct current, while the Raspberry Pi is required to manage data collection and storage. The GitHub page Mandeye Controller explains how to connect the open hardware (Będkowski, 2023). A video tutorial has also been added to the Mandeye Controller GitHub page, providing step-by-step instructions on assembling the components. Basic skills such as soldering wires and 3D printing prepared parts are required to assemble the system independently.

Figure 1 illustrates the basic workflow and connections within the Mandeye LiDAR system, highlighting its modular design and showing how the components are connected.

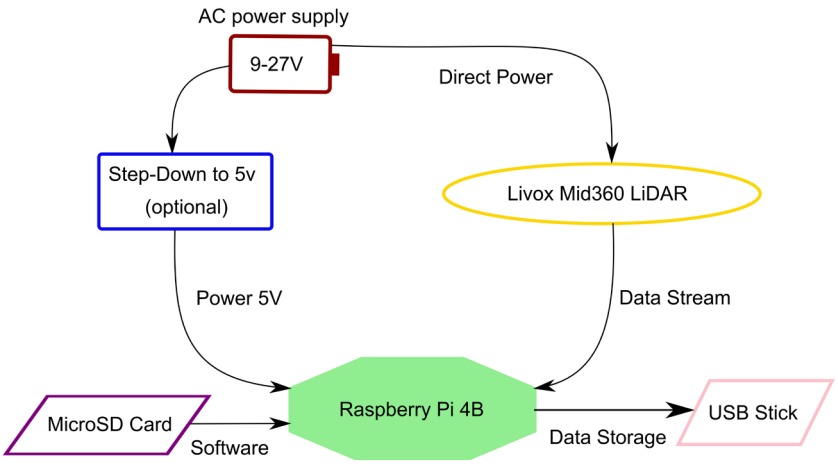

Fig. 1. Simplified scheme of the Mandeye LiDAR system.

Adaptation for speleological applications

Once assembled, the system can be configured for speleological applications, either as a handheld device for navigating narrow passages or mounted on a helmet for hands-free operation. These configurations make the Mandeye system adaptable to various cave exploration scenarios. Figure 2 demonstrates these configurations.

Fig. 2. Mandeye LiDAR system for mobile cave mapping: the handheld version for confined spaces (left) and the helmet-mounted version for hands-free operation in larger cave sections (right).

Speleology is usually a non-profit activity, relying on the efforts of voluntary cavers. As a result, speleological associations cannot allocate significant funds for surveying equipment. The Mandeye system is based on open hardware and open-source software technologies, making it much more affordable than commercial alternatives such as Geoslam (Domazetović et al., 2024), Greenvalley (Zhang et al., 2024), and Gexcel (Vassena & Clerici, 2018). The Mandeye system can be assembled for less than 1,000 EUR, making it affordable for most speleological associations today.

Point cloud preparation

During speleological surveys, the Mandeye system collects raw data in CSV and LAZ formats, which are then processed using the open-source HDMapping software. The software, available on the GitHub page

MapsHD/HDMapping (Będkowski, 2022a) provides tools for performing figure closure, splitting paths into smaller segments, and merging multiple scans into a single dataset. Geo-referencing is performed using GNSS data or known reference points to ensure precise alignment of scans. The mathematical foundation that served as the basis for software development is described in Będkowski (2022b).

A significant contribution of our approach is the multi-session data registration and georeferencing, which enables combining scans from different sessions into one cohesive point cloud. Single-session processing organizes LiDAR/IMU data into consecutive poses that form a trajectory. LiDAR odometry, a well-established term in LiDAR-IMU systems, estimates the sensor's trajectory by analyzing sequential point clouds and IMU data, enabling precise alignment of consecutive poses. These poses are then optimized using pose graph SLAM (Grisetti et al., 2010) with a key modification – the rotation matrix is parameterized using Tait-Bryan angles. This allows for intuitive uncertainty assignment to rotations along each axis, enhancing accuracy. This approach supports the integration of multiple datasets collected over extended periods, making it particularly useful for long-term speleological surveys.

While most open-source solutions run on Linux OS, Mandeye operates on Windows, which significantly simplifies usage for a larger number of users.

The workflow for processing data with HDMapping consists of three main steps, each performed using dedicated software tools:

1. Creating a trajectory and merging scans: Using lidar_odometry_step_1.exe, individual scans are aligned and merged into a connected point cloud.
2. Figure closure, georeferencing, and splitting: Multi_view_tls_registration_step_2.exe supports figure closure, georeferencing to known points, and splitting large datasets into smaller sections for easier processing.
3. Merging datasets: Finally, multi_session_registration_step_3.exe enables merging smaller datasets into large, unified point clouds for comprehensive analysis.

In large cave systems, figure closure can be used to align the point cloud and refine the trajectory. When figure closure is unavailable, independent control measurements can be employed to determine traverse points, which can be used for georeferencing the point cloud and partially for verifying deviations. These measurements can be performed in ways familiar to speleologists, such as developing the traverse using a compass, clinometer, and distance measurements. This is further elaborated in the section discussing data processing and profile generation.

The open-source software CloudCompare (CloudCompare, n.d.) is frequently used for advanced data processing tasks, such as manually cleaning point clouds, applying filters (e.g., statistical outlier removal (SOR), and generating longitudinal and cross-sectional profiles. While HDMapping provides essential tools for generating and visualizing point clouds, CloudCompare complements it by offering a broader range of specialized functions for refining and analyzing the data. This combination ensures efficient and flexible data processing tailored to the needs of speleological surveys.

In the following section, the Mandeye system will be compared to similar softwares available on the market.

COMPARISON TO SIMILAR STATE-OF-THE-ART SYSTEMS

To place our solution within the current state-of-the-art context, we gathered relevant features of key systems in Table 1. To provide a meaningful comparison, the systems included in this study were selected based on several criteria: their significant influence in LiDAR-IMU-based mapping and localization, their frequent citation in state-of-the-art research, and their foundational role in developing newer algorithms. While some of these systems, such as Zebedee (Bosse et al., 2012) and LOAM (Zhang & Singh, 2014), may not be the most recent, they remain highly relevant as benchmarks due to their groundbreaking contributions and continued use in evaluating modern approaches. The compared systems include Zebedee (Bosse et al., 2012), LOAM (Zhang & Singh, 2014), LeGO-LOAM (Shan & Englot, 2018), LIO-SAM (Shan et al., 2020), FAST-LIO (Xu & Zhang, 2021), FAST-LIO2 (Xu et al., 2022), and RI-LIO (Zhang et al., 2023). All these algorithms integrate IMU and LiDAR, facilitating robust mapping and localization.

Our approach is modular, providing algorithms for loop closure using techniques such as edge error minimization with ICP (Iterative Closest Point) or NDT (Normal Distributions Transform). Additionally, we offer automatic loop closure for small error corrections, while manual loop closure is available for larger errors.

A key difference compared to other LiDAR odometry algorithms is the use of the Madgwick filter for initial rotation calculation (Madgwick et al., 2011), which is a sensor fusion algorithm that estimates orientation by integrating data from accelerometers, gyroscopes, and (optionally) magnetometers. Our system provides accurate initial rotation estimates, ensuring robust LiDAR and IMU data integration. This process allows robust trajectory alignment and significantly enhances the accuracy of the subsequent optimization processes, such as pose graph SLAM, alongside the Gaussian representation of 3D geometry. This representation models the uncertainty of 3D points and surfaces as probability distributions, capturing the variability and noise inherent in LiDAR measurements. By doing so, it allows for more precise alignment and optimization of point clouds during the integration process. Combined with multi-session alignment, these methods are particularly suitable for large-scale projects. Unlike most other algorithms, which primarily operate in real time, our approach performs calculations during post-processing. This means that data are collected during the survey, while the mapping process is completed afterward. This allows us to detect errors and achieve greater accuracy in the final results.

Table 1. Comparison of state-of-the-art LiDAR mobile mapping systems.

Method	Year	Loosely coupled	Tightly coupled	IMU filter	ICP	NDT	Features	Loop closure (pose graph optimization)	Loop closure (point cloud refinement)	Single session	Multi session	Georefe-rencing	Open source	Open hardware	Real time
Zebedee	2012		Yes				surfels		Yes	Yes					
LOAM	2014	Yes					line, plane	Yes		Yes			Yes		Yes
LeGO-LOAM	2018	Yes					planar, edge	Yes		Yes			Yes		Yes
LIO-SAM	2020		Yes				planar, edge	Yes		Yes		Yes	Yes		Yes
FAST-LIO	2021		Yes	EKF			planar, edge			Yes			Yes	Yes	Yes
FAST-LIO2	2022		Yes		Yes		plane			Yes			Yes		Yes
RI-LIO	2023		Yes		Yes		plane, reflectivity			Yes			Yes		Yes
This study	2024	Yes	Yes	Madgwick	Yes	Yes	Gaussian	Yes	Yes	Yes	Yes	Yes	Yes	Yes	

SURVEYING OF GORNJA BARAĆEVA CAVE THROUGHOUT HISTORY

Gornja Baraćeva Cave in Croatia was selected to test the capabilities and accuracy of the described surveying system.

Croatia has approximately 10,000 known caves (Hrvatski Planinarski Savez, n.d.). Around 30 have been adapted for tourist visits (Božić, 2019). Gornja Baraćeva Cave is one of Croatia's most visited show caves (Fig. 3).

The Barać Caves were first described in literature in 1885 and have since been frequently mentioned in various publications over a long period. Several speleological maps have been created during this time. More detailed information about the history of the exploration of the Barać Caves can be found in (Božić, 2014).

Only the entrance section of Gornja (Upper) Baraćeva Cave, extending 140 m, is open to tourists.

To virtually introduce visitors to the remaining, not easily accessible areas of the cave, 3D static laser scans of the Upper and Donja (Lower) Barać Caves were acquired. This work was part of the European project Speleon — Center for Underground Heritage.

The field survey was conducted at the end of 2022. Using GNSS and a total station (Fig. 4), a surface geodetic network was established connecting the entrances of Gornja and Donja Caves. Precise polygonal traverses were also developed within both caves using the total station. These polygonal traverse points were used to geo-reference the static scans.

Three to five people were involved in the field survey of both caves, working for 12 full days, averaging 14 hours daily. The processing of the results took approximately as long as the field measurements but with one to three people working on it. The Faro Focus 3D X330 HD scanner was used to scan the tourist section of Gornja Baraćeva Cave, while the Leica BLK 360 scanner was used for other sections that were narrower and more difficult to navigate.

The resulting 3D models can be viewed at the Speleon Center, near the Barać Caves entrance (Speleon, n.d.).

Since high-quality and expensive equipment was used in this case, and significant effort was dedicated for data collection and processing, the applied methods and instruments typically achieve accuracy within a few centimeters. However, since the survey involved a blind polygonal traverse, it is impossible to determine its exact accuracy. Nevertheless, the results can be considered error-free compared to the methods used later, conducted with inherently less accurate instruments (e.g., DISTO X compared to a total station) and generally less precise methods, such as dynamic scanning compared to static scanning.

SURVEY OF GORNJA BARAĆEVA CAVE USING THE MANDEYE LIDAR SYSTEM

A larger section of Gornja Baraćeva Cave was resurveyed on July 19th 2024, using the Mandeye mobile LiDAR system. The surveying process was

smooth and fast, with the measurements being taken at the pace of walking through the cave. It was sufficient to press a single button and walk through the cave while the system recorded the data.

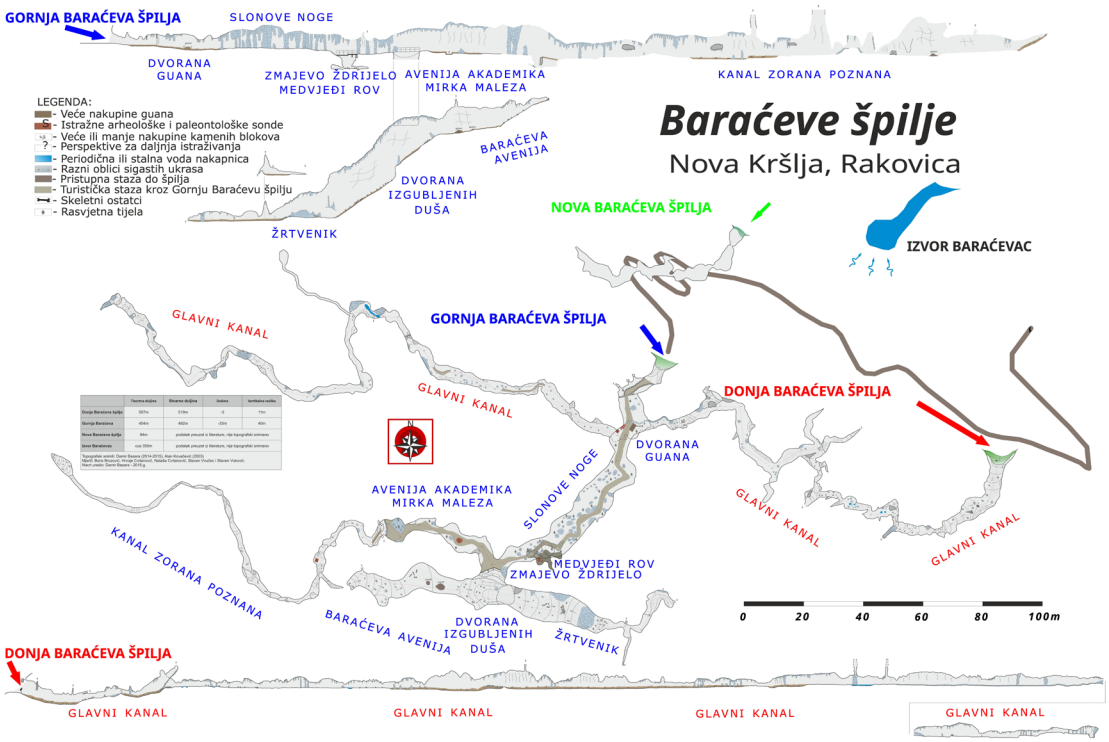

Fig. 3. Speleological map of the Barać Caves from 2015.

Fig. 4. Survey conducted in 2022. on the left - using a total station, and on the right - using a static laser scanner (Leica BLK 360).

To better georeference the final scan, we positioned the Mandeye system at each polygonal station in the tourist section, where the coordinates had been determined during the 2022 survey. While it is not strictly necessary to use both methods for creating high-quality 3D models of caves, we recommend their combined use. Cavers are generally familiar with developing polygonal traverses and can perform these quickly and accurately in the field. This approach ensures a higher overall accuracy of the cave model. Relying solely on georeferencing at the entrance reduces accuracy, while the absence of georeferencing altogether results in a model that is not properly oriented in space, limiting its usability. As shown in Figure 5A, the trajectory of the Mandeye system was mapped through the tourist section of the cave.

From the side view, it is visible that the LiDAR system was physically lowered as close as possible to each Ground Control Point (GCP) to ensure higher accuracy during the georeferencing of the final scan (Fig. 5B). These GCPs correspond to the polygonal traverse points determined during the 2022 survey. Although this lowering is important for georeferencing, it has some undesired effects, such as lengthening of the trajectory, which can later negatively impact the creation of cross-sections and the animations of movement through the cave. For this reason, the trajectory was edited, i.e., unnecessary parts were removed. In addition to the vertical extension, the path was also elongated horizontally because one part of the cave contains many stalagmites and columns (Fig. 5C).

The trajectory was elongated to move around the stalagmites and columns to capture this complex part of the cave in as much detail as possible. This approach ensured better coverage of cave features that would otherwise remain invisible in the 3D point cloud if the LiDAR passed only on one side. These parts were also edited to avoid causing issues during later data processing, which will be discussed later in the article.

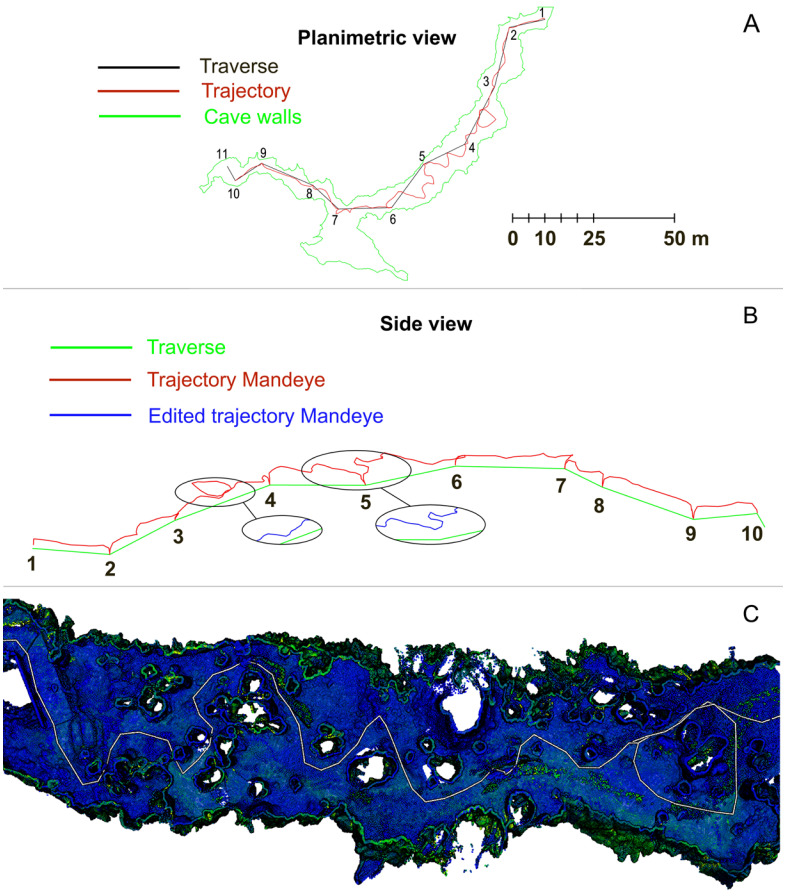

Fig. 5. A. Planimetric view of the tourist section of the cave; B. Trajectory and polygonal traverse shown from a side view; C. Moving through a complex area of Gornja Baraćeva Cave.

Survey using the DistoX2 system

Since speleologists generally do not use total stations due to their high cost, burden, and time requirements, the traverse points in the tourist section were observed using the DistoX2, a specific model of the DistoX family that is widely used in everyday speleological practice because it is portable and efficient. In this study, the total station survey served as a reference to assess the accuracy of polygonal traverse points obtained with the DistoX2. Developing a polygonal traverse with DistoX2 is very fast (slightly slower than walking speed). Figure 6 shows that an error occurred when sighting from point 6 to point 7.

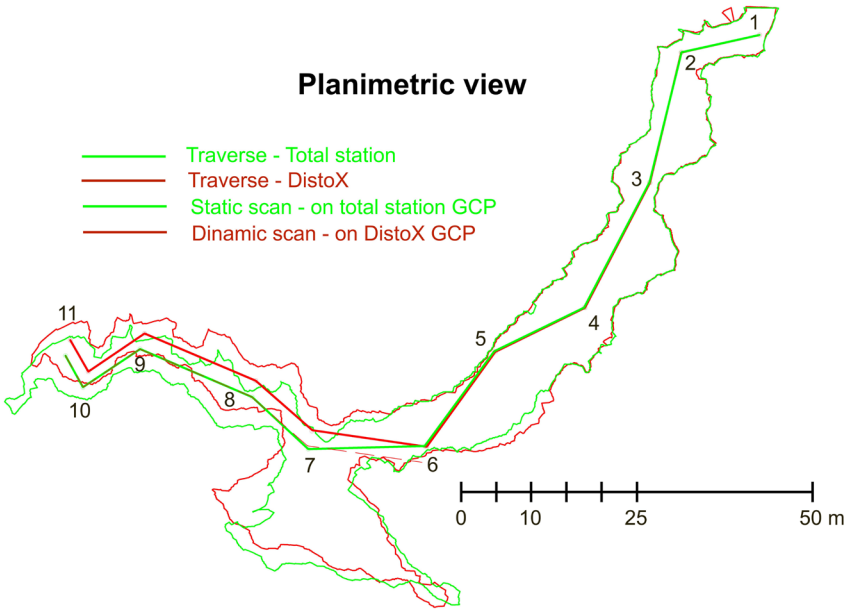

Fig. 6. Comparison of the ground plan and polygonal traverse obtained using the total station and DistoX.

During the survey in that section, there were tourist visitors present, and there was also light, so it is possible that something interfered with the electronic compass, leading to magnetic anomalies and poor results. This can also happen in everyday speleological practice when the surveyor brings the device too close to batteries, carabiners, or other metal objects. Otherwise, the GCPs obtained using the DistoX2 system align quite well with the GCP points obtained via the total station.

Figure 6 shows that the ground plan generated from the dynamic scan aligns well with the ground plan of the cave wall obtained from the static scan in the area where the GCP points match. However, if the azimuth is determined incorrectly, it results in inaccurate determination of the GCP coordinates and, consequently, incorrect georeferencing of the dynamic scan, causing the entire remaining ground plan to rotate by the magnitude of the error.

Since the proposed new surveying approach, which integrates classical speleological techniques with low-cost mobile LiDAR mapping, significantly speeds up and simplifies the process, it may be a good practice to observe polygon traverse points in two directions: one towards the end of the cave and the other from the end back towards the cave entrance. If discrepancies arise at any point, the trajectory from the dynamic scan can be used to determine which of the two measurements is correct.

Table 2 provides data related to the duration of the survey and the total surveyed length obtained using different systems.

Table 2. Time required and distance covered for different survey methods.

Method	Survey time	Length (m)	Edited length (m)
Classical Speleological Survey	~300 min	140.60	
Traverse - total station	~200 min	140.32	
Laser Scanning	~300 min	~150	
Traverse - DistoX2	~10 min	139.72	
Trajectory - Mandeye scan 09	~17 min	206.21	170.10

Using the Mandeye system, 122,130,805 points were collected only in the tourist section. This vast amount of data made it possible to clearly distinguish different objects in the cave based on the point cloud, colored according to signal return intensity (Fig. 7).

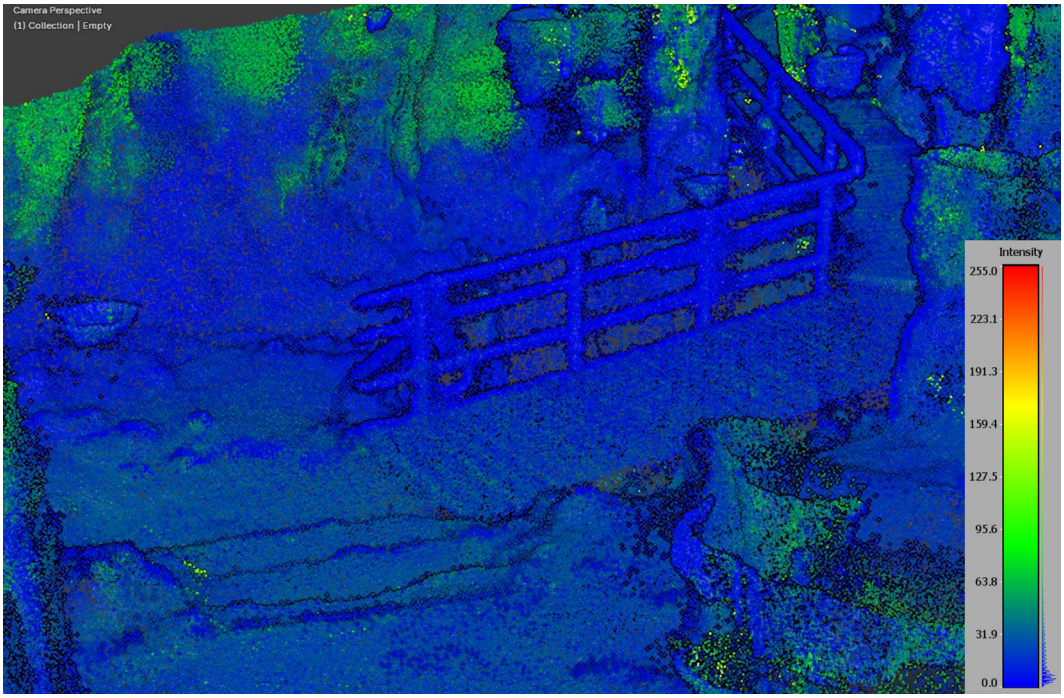

Fig. 7. Point cloud colored based on signal return intensity.

Comparison of point clouds and analysis of results

This section focuses on comparing the point clouds obtained from dynamic and static scans, as well as the analysis of the deviations and resulting accuracy. The goal is to evaluate the performance of the dynamic scan relative to the static scan based on the processed data and visualizations.

To speed up further data processing, the dense point cloud was subsampled by retaining points every 3 cm, and the same was done with the static scan obtained in the 2022 survey. The distances between the point clouds were calculated using the Cloud-to-Cloud (C2C) distance computation tool within CloudCompare software, which measures deviations in the spatial

positions of points between two point clouds. These deviations indicate how closely the points in the target cloud align with the reference cloud. The results are visualized through a color-coded map to highlight variations. Figure 8A graphically shows the deviations of the Mandeye scan compared to the static scan.

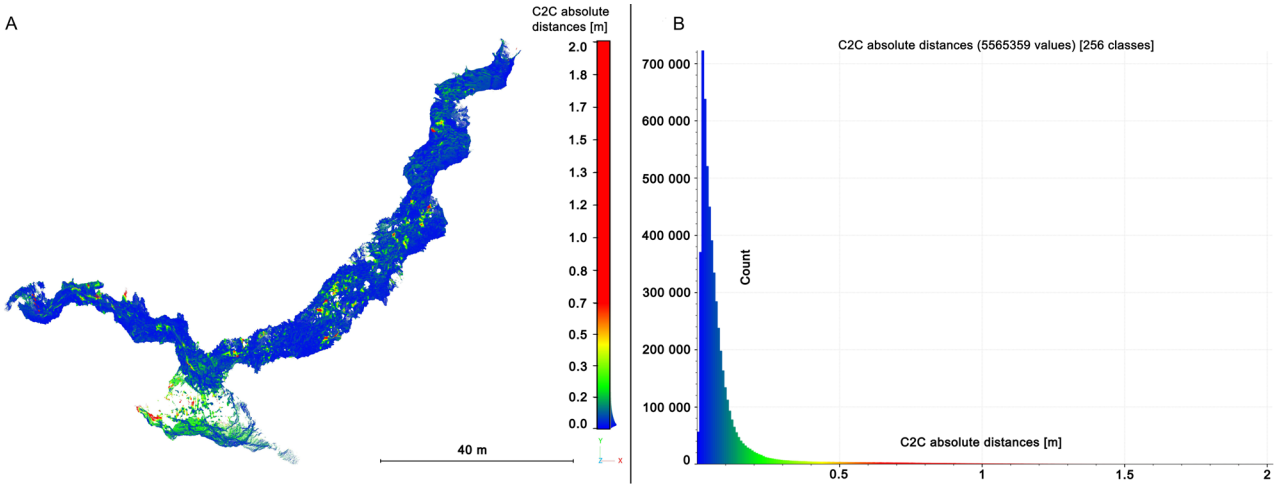

Fig. 8. A. Differences between the static and dynamic scans; B. Histogram of length deviations between two point clouds.

From the image, it is evident that most differences are within 15 cm (blue color), while some parts differ by up to half a meter (green color), with only a few areas deviating by more than half a meter (red color). Visual inspection revealed that these red discrepancies were primarily due to shadowing in the static scan. In dynamic scanning, there are significantly fewer shadows because data are collected from many more different angles, allowing the laser beams to penetrate behind obstacles more effectively. Therefore, dynamic scanning not only saves time but also provides better coverage of the scanned surfaces compared to the static method. In Figure 8B, these deviations are shown analytically, and it is evident that the vast majority of points differ by less than 25 cm.

Beyond the tourist section, we began scanning with the Mandeye system from the end of the cave towards the entrance. The red trajectory (Scan 16) represents the path from the end of the cave to just beyond a narrow section at point 25, while the blue trajectory (Scan 17) continues from this narrow section towards the cave entrance. These trajectories are illustrated in Figure 9A.

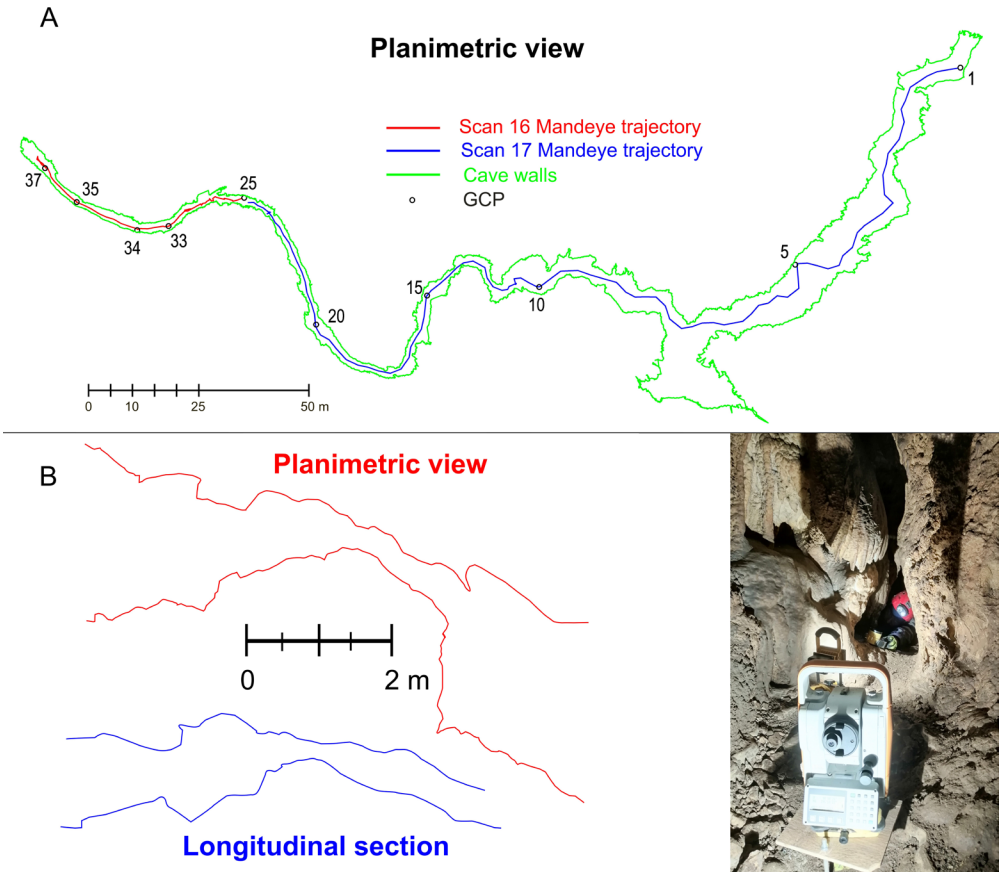

Fig. 9. A. Ground plan showing the trajectories followed through the cave; B. Narrow section near polygonal traverse point 25.

The final part of the cave is quite narrow and challenging to navigate, so the Mandeye system was only placed at points where conditions allowed. After the narrow part, the cave became more easy to navigate, and the Mandeye system was placed at every fifth point.

The cave's narrowest and most challenging part is from point 25 to the end. Figure 9B shows both the plan and section of this narrower part. In that very narrow and low part of the cave, approximately 3 meters long, the Mandeye system managed to collect data, but with somewhat greater deviations than in the rest of the cave.

Table 3 presents the statistical data related to individual scans 16 and 17 as well as their combined results. The data includes the time spent in the field, trajectory length, traverse length, and the number of points recorded.

The table shows that many points were collected in a relatively short period. Most importantly, the results are still quite consistent when the point cloud obtained using the Mandeye system is compared with the one obtained from static scanning.

Table 3. Statistical data related to individual scans 16 and 17, as well as their combined results.

Scan names	Time in the field (min.)	Trajectory length (m)	Traverse length (m)	Number of points
Scan 16	10.88	77.89	66.53	52,053,214
Scan 17	12.02	266.93	262.70	81,385,948
Scan 16 & 17	22.9	344.82	314.88	133,439,162

Figure 10A graphically shows the cloud-to-cloud deviations between the dynamic (Mandeye) scans and the static scan from 2022. Figure 10B analytically presents these deviations, demonstrating that most points still differ by less than 50 cm. The achieved accuracy is somewhat lower than in the tourist section but still within the generally acceptable limits for the speleological community.

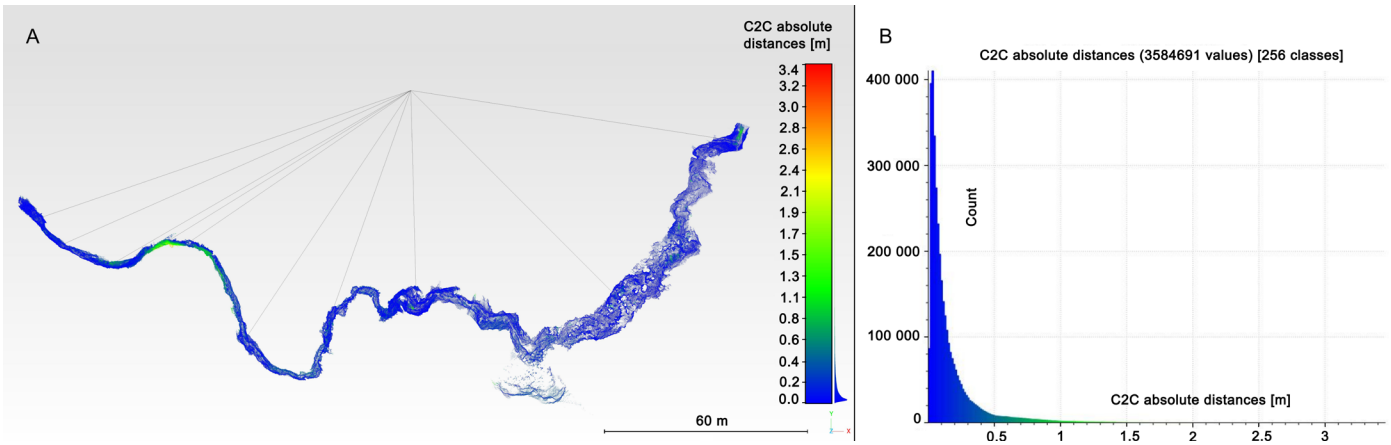

Fig. 10. A. Differences between dynamic scans and the static scan. B. Histogram of deviations between the dynamic and static scans.

Addressing accuracy in speleological surveys

While the achieved deviations in this study (25–50 cm) may not meet the stringent requirements of geo-engineering or technical LiDAR applications, they are generally acceptable within the speleological community. Cave surveying often involves highly challenging conditions, such as narrow passages, irregular geometry, and limited visibility, which inherently affect accuracy. Furthermore, traditional speleological surveys, particularly over longer traverses, frequently exhibit errors in the meter range due to cumulative deviations.

It is also important to note that cave surveying equipment is typically designed to be low-cost and compact, making it less accurate than high-end systems. The constraints of cave environments, such as narrow and low passages, necessitate small, portable devices that are easy to carry and operate.

We recognize the value of comparing results with other dynamic systems and plan to conduct such comparisons as affordable new sensors become available.

At today's level of development, an immediate transition to the complete application of 3D technology in caves is not realistic. It is more likely that there will be a transitional period during which the shift from 2D to 3D representation will gradually occur. Currently, most speleologists use analog 2D drawings for orientation in caves, and speleological cadasters also collect data in 2D. The following describes how, with the help of free software, a ground plan and a developed cave profile, ready to be submitted to cave cadasters, can be easily generated from a three-dimensional point cloud.

CREATING A GROUND PLAN

When we have a georeferenced 3D point cloud, generating a ground plan in CloudCompare software is straightforward. Detailed steps and the illustration of this procedure are provided in Supplementary Fig. S1. Using the methods explained in Supplementary Fig. S1, ground plans of the cave were generated both from the static scan and dynamic scanning using the Mandeye system.

Comparison of ground plans

The above-mentioned profiles were compared with each other, and the comparison also includes a ground plan obtained through traditional speleological

drawing. Figure 11 shows how the ground plan generated using the Mandeye system aligns quite well with the ground plan derived from the static scan. We can also observe that the ground plan created through traditional speleological drawing is roughly similar to those generated using LiDAR. To make the comparison possible, the traditional ground plan first had to be scaled using an analog scale.

Also, when measuring azimuth using a compass, the amount of magnetic declination must be taken into account. If the location and time of the surveying are known, it can be calculated online (National Oceanic and Atmospheric Administration, n.d.).

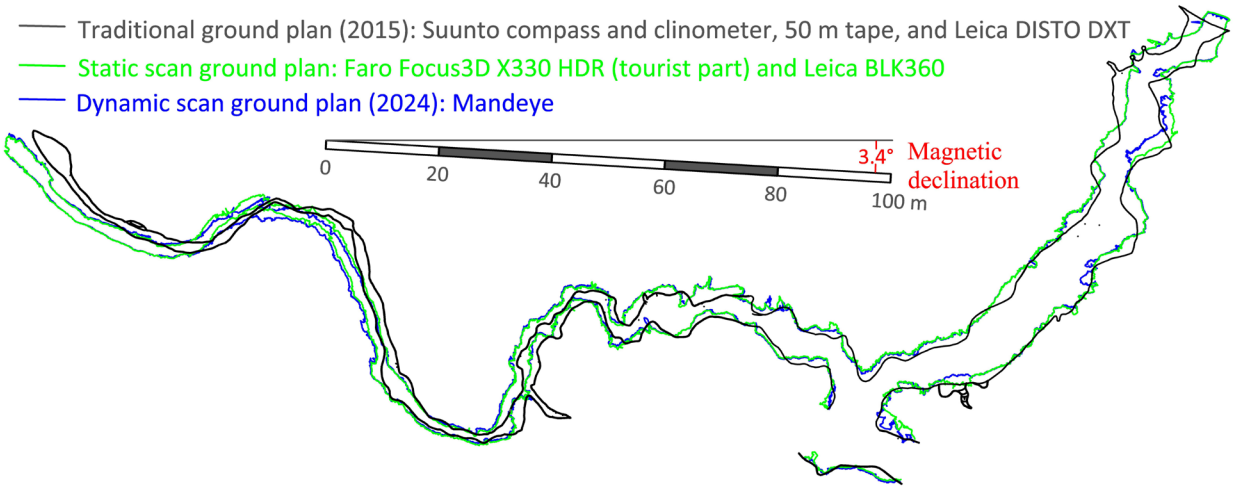

Fig. 11. Ground plan comparison.

GENERATING AN EXTENDED PROFILE

In addition to the ground plan, the extended profile is also very important for speleologists. The extended profile can also be obtained in the CloudCompare software, but the cave axis must be loaded in addition to the point cloud. A polygonal line or the trajectory along which the lidar system was moved can be used for the cave axis. The trajectory points recorded by the LiDAR system can be exported using the HDMapping software. Since the original trajectory contains a large number of points (200 points per second), a feature was introduced at the request of speleologists to make the export process more manageable. This feature allows users to export points at specific intervals (e.g., every 1 m or 5 m) instead of including all points. Additionally, it provides the option to increase the density of exported points in curved trajectory sections, which require greater detail to ensure the trajectory does not pass outside the cave walls. The trajectory points can be exported as a CSV file.

In addition to exporting the trajectory in CSV format, our software also supports direct export of the trajectory as a 3D polyline in DXF format. This functionality significantly simplifies the workflow, enabling users to immediately utilize the connected trajectory line in other software tools, such as CloudCompare.

Figure 12 illustrates the menu for exporting the trajectory as a 3D polyline in DXF format (2) and the associated parameters for controlling point reduction in the polyline (1).

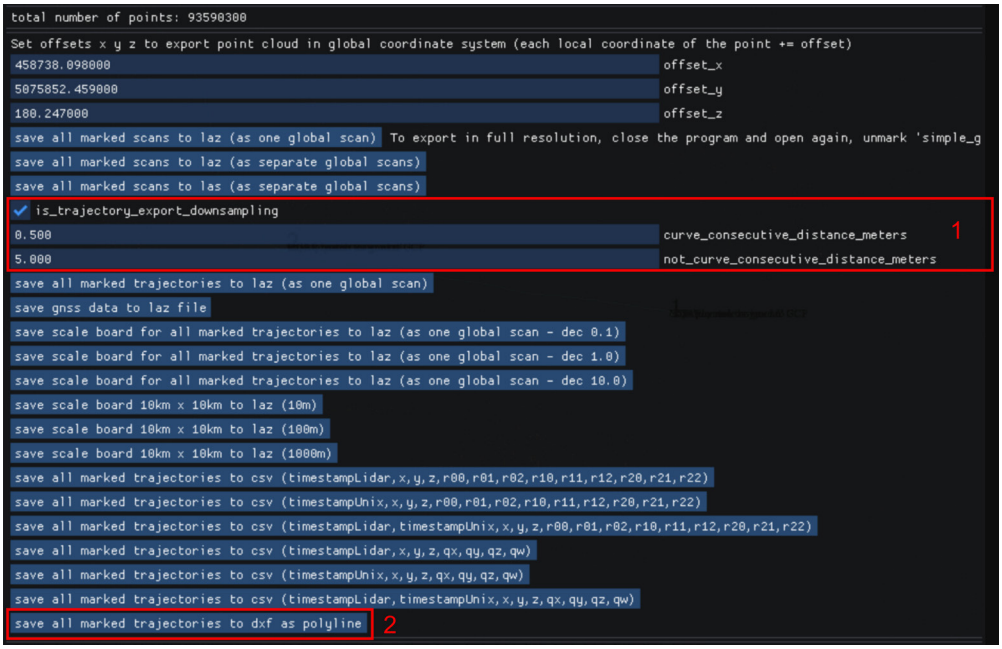

Fig. 12. Menu for exporting the trajectory as a 3D polyline in DXF format.

The DXF file you create can then be loaded into CloudCompare. Once you have the point cloud and trajectory or polygonal traverse loaded in CloudCompare, longitudinal cross-sections of the cave can be made by using a vertical plane along the trajectory to cut the point cloud. Similarly, the cave can be divided into two parts by intersecting the trajectory with a vertical plane, allowing one part to be excluded and the cave's interior to be viewed laterally. Additionally, the cave can be split into ceiling and floor sections by cutting the point cloud with a horizontal plane passing through the trajectory.

One feature significant for speleologists is the ability to generate an extended profile automatically. This process is detailed in Supplementary Figs S2, S3, and S4.

Extended profiles were created for the static and two dynamic scans using the abovementioned method. Figure 13A shows a comparison of the extended profiles.

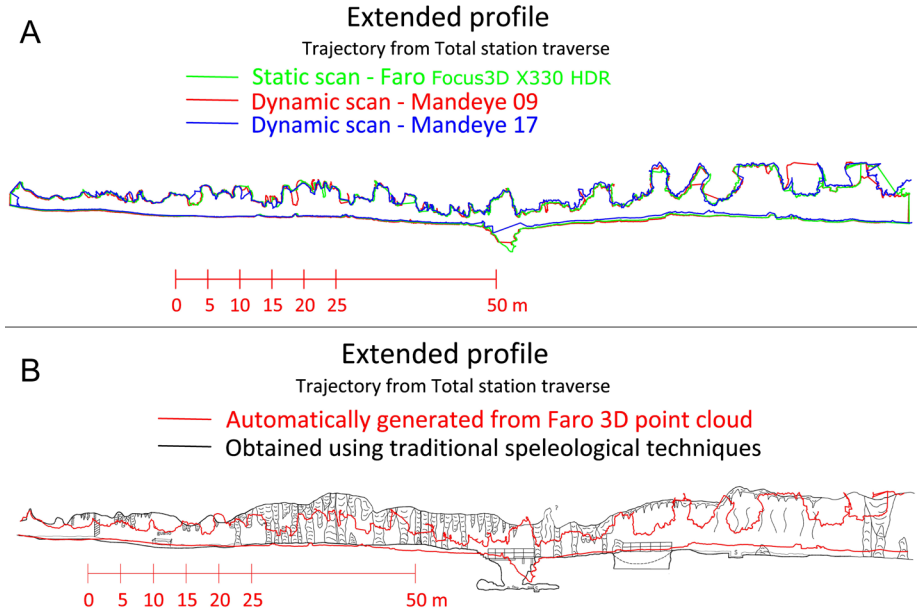

Fig. 13. A. Comparison of extended profiles for the Upper Barać Cave. B. Comparison of traditional and automatically generated extended profiles.

It also reveals that the extended profiles align pretty well overall. Slightly larger differences appear in a few locations, mainly because point clouds could not be obtained during scanning at those spots due to obstacles. Figure 13B shows a comparison between the extended profile obtained through the traditional speleological method and the mobile laser scanning method.

There are also similarities here, but certain slightly larger differences as well. These larger differences mainly arise because the path used to generate the extended profile from the 3D scan differs from the path used for the traditionally created extended profile. Additionally, the generated 3D profile is generally lower because it follows the vault height above the scanning trajectory. At the same time, in the traditional method, the speleologist typically draws the highest parts of the cave ceiling.

CROSS SECTIONS

Cross-sections in CloudCompare can be generated automatically, as explained in Supplementary Fig. S5, or manually, as described in Supplementary Fig. S6. When a C2C analysis is applied to the manually generated profiles from Supplementary Fig. S6, the absolute distances between the static and dynamic scans are shown in Figure 14.

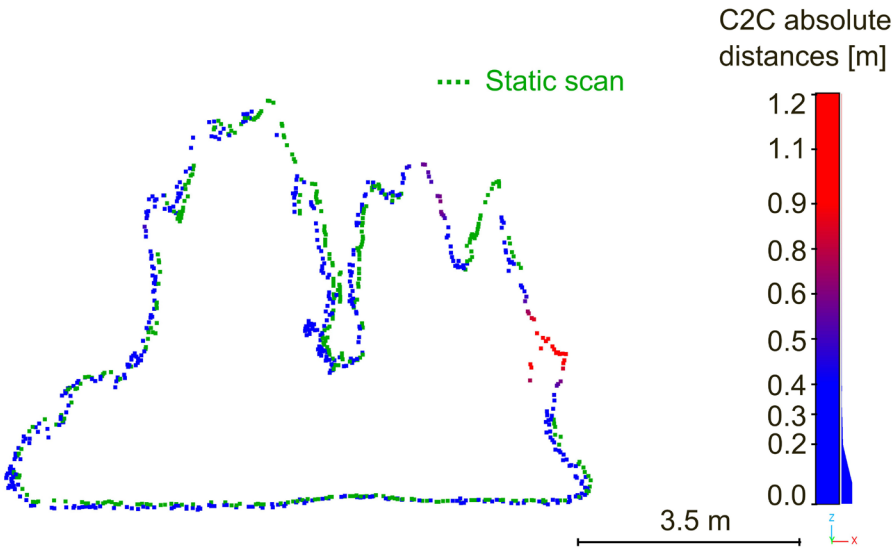

Fig. 14. C2C distances between static and dynamic scans for a cave cross-section.

The color scale on the right represents the magnitude of discrepancies, with blue indicating minimal differences and red indicating larger deviations. The larger deviations primarily occur in areas where the static scan failed to capture parts of the cave due to shadowing effects. In contrast, the dynamic scan provided more complete coverage. This highlights the advantages of dynamic scanning in capturing complex cave geometries with fewer occlusions (shadow zones).

CONCLUSIONS AND FUTURE WORK

Based on everything presented, we can conclude that mobile laser scanning can significantly simplify and speed up the survey of underground voids. A system based on open-source hardware and software, such as the Mandeye LiDAR, is affordable to the broader speleological community. This study shows that such hardware successfully collects data even in very narrow and low cave parts. Although very narrow and muddy passages, high chambers, and submerged sections remain challenging, technological advancements will likely resolve these issues soon.

The paper further demonstrates how, using free software, accurate and efficient ground plans and extended profiles can be generated from the collected data, forming the backbone of all other speleological research. In addition to extended profiles, the paper explains how cross-sections or any other types of sections can be generated. The additional effort invested in generating a path is worthwhile because that path can be used to crop point clouds or meshes created from the point cloud. It is also useful for creating extended profiles and can be very helpful when making animations where the camera moves through the cave along that path.

In future work, we will investigate a double LiDAR system to improve the performance and reliability of crawling, climbing, and other challenging cave scenarios. For this purpose, we will investigate a dual LiDAR system calibration procedure and ergonomic design to make cave surveying more reliable and to provide solutions for surveying in even more demanding conditions.

ACKNOWLEDGMENTS

We thank those who assisted during the 2022 survey. Marko Gojčeta, Čedo Josipović, and Grgur Hajdari contributed significantly through their hard work in developing the geodetic framework and static scanning of the Upper and Lower Barać Caves. This survey served as the basis for the comparisons presented in this paper. We also extend our thanks to Damir Basara and other cavers who participated in creating the 2015 speleological map for providing data used in comparing the results. Michał Pełka is thanked for his fundamental contribution in developing the hardware design. We are grateful to the reviewers for their constructive feedback, which greatly improved the quality of this manuscript.

Authorship statement: LR actively participated in the measurements, design, and writing of the article; AJ was involved in the measurements, provided constructive advice regarding the survey and software improvements, and contributed to the article; JB helped with hardware development, co-created the software, adapted it to speleologists' needs, and provided advice during measurements and article creation; JJ assisted with the article and actively participated in data analysis, image creation, and translating the article into English.

REFERENCES

Będkowski, J., 2022a. MapsHD/HDMapping. GitHub repository. https://github.com/MapsHD/HDMapping

Będkowski, J., 2022b. Large-scale simultaneous localization and mapping. Springer, Singapore, 308 p. https://doi.org/10.1007/978-981-19-1972-5

Będkowski, J., 2023. Mandeye Controller. GitHub repository. https://github.com/JanuszBedkowski/mandeye_controller

Bosse, M., Zlot, R., Flick, P., 2012. Zebedee: Design of a spring-mounted 3D range sensor with application to mobile mapping. IEEE Transactions on Robotics, 28(5), 1104-1119. https://doi.org/10.1109/TRO.2012.2200990

Božić, V., 2014. Speleološka istraživanja Baraćevih špilja. Subterranea Croatica, 12(17), 51-58. https://hrcak.srce.hr/file/411507

Božić, V., 2019. Speleološki turizam u Hrvatskoj. In: Rnjak, G. (Ed.), Speleologija II (Drugo izdanje). Hrvatski Planinarski Savez. https://sovelebit.wordpress.com/2019/04/16/speleologija-2-izdanje/

BRIC Survey Tool, n.d. BRIC5 Survey Tool. https://www.bricsurvey.com/

CloudCompare, n.d. Free 3D point cloud processing software. https://www.cloudcompare.org/

Corvi, M., n.d. TopoDroid 6.2.92-35. Mobile application software. http://marcocorvi.altervista.org/caving/speleoapps/speleoapks/TopoDroidApks.html

Domazetović, F., Lončar, N., Šaban, M., 2024. 3D mapping of karst caves using GeoSLAM technology: potentials and challenges. X Young Geomorphologists' Day, Venice. https://doi.org/10.13140/RG.2.2.25663.07845

Gáti, A., Rehány, N., Fekete, Z., Holl, B., Sűrű, P., 2016. Poor man's laser scanner: a simple method of 3D cave surveying. The CREG Journal, 96, 8-14. https://poormanslaserscanner.github.io/test_md/paper.pdf

Grisetti, G., Kummerle, R., Stachniss, C., Burgard, W., 2010. A tutorial on graph-based SLAM. IEEE intelligent Transportation Systems Magazine, 2(4), 31-43. https://doi.org/10.1109/MITS.2010.939925

Heeb, B., 2009. An all-in-one electronic cave surveying device. CREG Journal, 72, 8-10. https://paperless.bheeb.ch/download/DistoX.pdf

Heeb, B., 2014. The next generation of the DistoX: Cave surveying instrument. CREG Journal, 88, 5-8. https://paperless.bheeb.ch/download/DistoX2.pdf

Hrvatski Planinarski Savez, n.d. Speleologija. https://www.hps.hr/speleologija/

Kaňuk, J., Supinský, J., Meneely, J., Hochmuth, Z., Šašak, J., Gallay, M., Callieri, M., 2023. Laser Scanning of a complex cave system during multiple campaigns. In: Meneely, J. (Ed.), 3D Imaging of the Environment, CRC Press, Boca Raton, p. 56-81, https://doi.org/10.1201/9780429327575-4

Konstantinos, P.T., 2018. Paperless mapping and cave archaeology: a review on the application of DistoX survey method in archaeological cave sites. Journal of Archaeological Science: Reports, 18, 399-407. https://doi.org/10.1016/j.jasrep.2018.01.022

Li, N., Ho, C.P., Xue, J., Lim, L.W., Chen, G., Fu, Y.H., 2021. A progress review on solid-state LiDAR and nanophotonics-based LiDAR sensors. Laser & Photonics Reviews, 16(11), e202100511. https://doi.org/10.1002/lpor.202100511

Madgwick, S.O., Harrison, A.J., Vaidyanathan, R., 2011. Estimation of IMU and MARG orientation using a gradient descent algorithm. In: 2011 IEEE International Conference on Rehabilitation Robotics, 1-7. https://doi.org/10.1109/ICORR.2011.5975346

National Oceanic and Atmospheric Administration, n.d. Geomagnetic calculator. https://www.ngdc.noaa.gov/geomag/calculators/magcalc.shtml

Sevil-Aguareles, J., Pisani, L., Chiarini, V., Santagata, T., De Waele, J., 2025. Gypsum cave notches and their palaeoenvironmental significance: A combined morphometric study using terrestrial laser scanning, traditional cave mapping, and geomorphological observations. Geomorphology 471, 1-13. https://doi.org/10.1016/j.geomorph.2024.109576

Shan, T., Englot, B., 2018. LEGO-LOAM: Lightweight and ground-optimized lidar odometry and mapping on variable terrain. In: 2018 IEEE/RSJ International Conference on Intelligent Robots and Systems (IROS), 4758-4765. https://doi.org/10.1109/IROS.2018.8594299

Shan, T., Englot, B., Meyers, D., Wang, W., Ratti, C., Rus, D., 2020. LIO-SAM: Tightly-coupled LiDAR inertial odometry via smoothing and mapping. In: 2020 IEEE/RSJ International Conference on Intelligent Robots and Systems (IROS), 5135-5142. https://doi.org/10.1109/IROS45743.2020.9341176

Silvestre, I., Rodrigues, J.I., Figueiredo, M., Veiga-Pires, C.C., 2015. High-resolution digital 3D models of Algar do Penico Chamber: limitations, challenges, and potential. International Journal of Speleology, 44(1), 25-35. https://doi.org/10.5038/1827-806X.44.1.3

Speleon – Center for underground heritage. https://barac-caves.com/visit-speleon/

Šupinský, J., Kaňuk, J., Nováková, M., Hochmuth, Z., 2022. LiDAR point clouds processing for large-scale cave mapping: A case study of the Majko dome in the Domica cave. Journal of Maps, 18(2), 268-275. https://doi.org/10.1080/17445647.2022.2035270

Therion Development Team, n.d. http://therion.speleo.sk/

Tian, S., 2023. DistoXBLE. Facebook page. https://www.facebook.com/siwei.tian.7/

Tringali, L., Canciani, G., Debenjak, A., Tripari, T., 2024. Charlotte: A modern tool for cave surveying. International Journal of Speleology, 53(3), ijs2496. https://doi.org/10.5038/1827-806X.53.3.2496

Trybała, P., Kasza, D., Wajs, J., Remondino, F., 2023. Comparison of low-cost handheld LiDAR-based SLAM Sstems for mapping underground tunnels. ISPRS Archives, XLVIII-1-W1-2023, 517-524. https://doi.org/10.5194/isprs-archives-XLVIII-1-W1-2023-517-2023

Vassena, G., Clerici, A., 2018. Open pit mine 3D mapping by TLS and digital photogrammetry: 3D model update thanks to a SLAM-based approach. ISPRS Archives, XLII-2, 1145-1148. https://doi.org/10.5194/isprs-archives-XLII-2-1145-2018

White, W.B., 2019. Surveying caves. In: White, W.B., Culver, D.C., Pipan, T. (Eds.), Encyclopedia of caves, Elsevier/Academic Press, New York, p. 911-916. https://doi.org/10.1016/B978-0-12-814124-3.00123-0

Xu, W., Zhang, F., 2021. FAST-LIO: A fast, robust lidar-inertial odometry package by tightly-coupled iterated Kalman filter. IEEE Robotics and Automation Letters, 6(2), 3317-3324. https://doi.org/10.1109/LRA.2021.3064227

Xu, W., Cai, Y., He, D., Lin, J., Zhang, F., 2022. FAST-LIO2: Fast direct lidar-inertial odometry. IEEE Transactions on Robotics, 38(4), 2053-2073. https://doi.org/10.1109/TRO.2022.3141876

Zlot, R., Bosse, M., 2014. Three-dimensional mobile mapping of caves. Journal of Cave and Karst Studies, 76(3), 191-198. https://doi.org/10.4311/2012EX0287

Zhang, C., Chen, J., Li, P., Han, S., Xu, J., 2024. Integrated high-precision real scene 3D modeling of karst cave landscape based on laser scanning and photogrammetry. Scientific Reports, 14, 20485. https://doi.org/10.1038/s41598-024-71113-y

Zhang, J., Singh, S., 2014. LOAM: Lidar odometry and mapping in real-time. In: Fox, D., Kavraki, L.E., Kurniawati, H. (Eds.), Robotics: Science and Systems Conference, 2(9), 1-9. https://doi.org/10.15607/RSS.2014.X.007

Zhang, Y., Tian, Y., Wang, W., Yang, G., Li, Z., Jing, F., Tan, M., 2023. RI-LIO: Reflectivity image assisted tightly-coupled lidar-inertial odometry. IEEE Robotics and Automation Letters, 8(3), 1802-1809. https://doi.org/10.1109/LRA.2023.3243528